A Novel Nonlinear Modeling and Dynamic Analysis of Solenoid Actuated Butterfly Valves Coupled in Series

Peiman Naseradinmousavi
Assistant Professor
Department of Mechanical Engineering,
San Diego State University (SDSU),
San Diego, CA 92115
e-mail: peiman.naseradinmousavi@villanova.edu

In this paper, we focus on a novel nonlinear modeling and dynamic analysis of the actuated butterfly valves coupled in series. The actuated valves used in the chilled water systems of the U.S. Navy and commercial ships, namely, "smart valves," recently have received much attention when many of them are operating in a complex network. The network regulates the pressure of the pipeline, while several nonlinear torques/forces including the hydrodynamic and bearing torques and the magnetomotive force affect the performance of each set individually and subsequently the whole system via the couplings among the valves. The contribution of this work is to model such couplings in the presence of the nonlinearities and an applied periodic noise and then carry out dynamic analysis of the valves. We examine the model developed with/without actuation by applying a periodic noise on the upstream valve to capture the couplings among the parameters of both the actuators and valves. This would help us predict the behavior of a particular valve in the network subject to motions of other valves.
[DOI: 10.1115/1.4027990]

1 Introduction

We previously developed a comprehensive dynamic model [1–4] of a solenoid actuated butterfly valve as a part of an enormous fluid network of the U.S. Navy ships and submarines [5–7]. The smart valve research we carried out is a critical element of the chilled water systems used in cooling applications affecting different components like radar and sonar systems. The dynamic model was developed to describe the interdisciplinary physics of the set including electromagnetics, fluid mechanics, and mechanical elements. Magnetic actuators are used in various applications including macroscale and microscale devices [8,9] for developing medical, engineering, and transportation tools. Some efforts have been made for synchronizing electromechanical systems in a unidirectional coupling or in a network configuration [10–13] where very few contributions have been reported for accurate nonlinear analysis of the actuated valves coupled in series due to the complexity of the whole system. Obviously, this work can be utilized in a wide range of researches including bioengineering, medicine, and engineering fields. The model developed here consists of two actuated valves though the method utilized, promisingly, can be used in developing a general nonlinear model including several valves and actuators.

Undoubtedly, some simplifying assumptions were hence needed to be applied to avoid worthless complexity by ignoring the magnetic diffusion, fringing, and flux leakage of the solenoid actuator [1]. Clearly, the diffusion time is too sensitive to the applied current of the actuator such that a high value of the current yields a negligible diffusion time and vice versa; we use the current of 4(A) yielding the diffusion time of 20 ms for the Bessho actuator [14]. Note that the plunger of the solenoid actuator is motionless during the diffusion time; there is no powerful magnetic force to move the plunger. Another assumption is to utilize laminar flow making us able to model the system analytically (this has been a common practice to avoid the complexity of numerical approach for the turbulent regime); the flow torques including the hydrodynamic and bearing torques have been formulated based on the laminar regime [1,15–17]. We apply those assumptions here while the coupled system is too complex by itself.

A nonlinear dynamic analysis we then carried out for a set of the valve/actuator to capture dangerous behaviors including transient chaos and crisis [2]. Other results we have reported [4] include quintessentially nonlinear dynamic behavior; a single butterfly valve oscillates due to the supply voltage containing a DC component and a time varying component which can be modeled as a sinusoidal noise. The source of the oscillation applied on the upstream valve here is assumed to be mechanical in order to evaluate its effects on the downstream valve for both the steady and moving phases. We also optimized the system design and operation in order to save the amount of energy used (upward of 41%) and increase the set performance [3].

We mainly deal with two cases: (1) without actuation and (2) with actuation. For the first case, we apply the periodic noise at the steady position of the upstream valve to investigate what is expected to occur for the downstream valve. The latter one discusses the valves' motions coupled by the nonlinear magnetic parameters in order to consider the effects of a disturbed valve on another.

2 Mathematical Modeling

Figure 1(*a*) presents two actuated valves in series and Fig. 1(*b*) shows a simple model (schematic) of the unactuated valves held in certain opening angles (α_1 and α_2) with the aid of constant torques, $T_{\text{ho}i}$. The system here consists of two solenoid actuators energized by electric voltages (DC or AC) which move the plungers. The plungers are connected to butterfly valves through the racks and pinions as shown in Fig. 1(*a*). For both the sets, the magnetic flux generates the needed electromagnetic force to move the plunger and subsequently results in the rotation of the butterfly valve with the aid of the rack and pinion mechanism. Note that we utilized a return spring for the valve opening; this is a common practice among manufacturers. Both the valves are subject to the nonlinear torques including the hydrodynamic (T_h) and bearing torques (T_b). We neglect the constant and small seating torque. We begin to model the flow line as three resistors obviously two of them as changing ones for the opening/closing valves and the middle one as a constant resistor. Note that the inlet and outlet pressures are supposed to be known. Assuming the laminar flow, the Hagen–Poiseuille [18] formula states the pressure drop between two valves (points 1 and 2) as follows:

$$P_1 - P_2 = \underbrace{\frac{128\mu_\text{f} L}{\pi D_\text{v}^4}}_{R_\text{L}} q_\text{v} \tag{1}$$

where μ_f is the fluid dynamic viscosity, D_v indicates the valve diameter, q_v is the volumetric flow rate, L is the pipe length between two valves, and R_L is the constant resistance. Typically, the regulating valves including butterfly ones deal with two important parameters, namely, the valve's "resistance (R)" and "coefficient (c_v)," The valve resistance, which depends on the valve rotation angle as well as the valve coefficient, is calculated as follows [19]:

$$R_i(\alpha_i) = \frac{891 D_\text{v}^4}{c_{\text{v}i}^2(\alpha_i)}, \quad i = 1, 2 \tag{2}$$

Contributed by the Dynamic Systems Division of ASME for publication in the Journal of Dynamic Systems, Measurement, and Control. Manuscript received September 19, 2013; final manuscript received June 25, 2014; published online August 28, 2014. Assoc. Editor: Yang Shi.

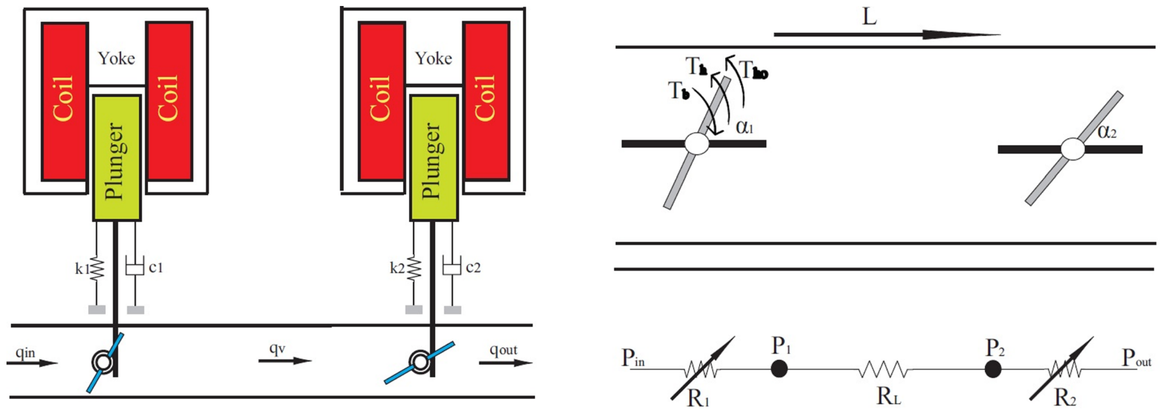

(a) (b)

Fig. 1 (*a*) Two actuated butterfly valves in series. (*b*) A model of two valves in series without actuation.

where c_v is the valve coefficient depending on the valve rotation angle. The pressure drop across the valve is expressed as follows [17]:

$$\Delta P_i(\alpha_i) = 0.5 R_i(\alpha_i)\rho v^2 \tag{3}$$

where v is the flow velocity and ρ indicates the density of the media. Rewriting Eq. (3) yields

$$\Delta P_i(\alpha_i) = \underbrace{\frac{\pi^2 D_v^4 v^2}{16}}_{q_v^2} \underbrace{\frac{8\times R_i(\alpha_i)\rho}{\pi^2 D_v^4}}_{R_{ni}(\alpha_i)} = R_{ni}(\alpha_i) q_v^2 \tag{4}$$

The pressure drop of Eq. (4) is used in both the hydrodynamic and bearing torques' formulations. The hydrodynamic torques [17] of both the valves are calculated as follows:

$$T_{hi} = \frac{16 T_{ci}(\alpha_i) D_v^3 \Delta P_i}{3\pi\left(1 - \dfrac{C_{cci}(\alpha_i)(1-\sin(\alpha_i))}{2}\right)^2} = f_i(\alpha_i) D_v^3 \Delta P_i \tag{5}$$

where $f_i(\alpha_i) = (16T_{ci}(\alpha_i)/3\pi(1-(C_{cci}(\alpha_i)(1-\sin(\alpha_i))/2))^2)$. T_{ci} and C_{cci} are the hydrodynamic torque and the sum of upper and lower contraction coefficients which depend on the valve rotation angle [1]. The bearing torque, as a resistance torque opposing the valve motion, is obtained as follows [20]:

$$T_{bi} = 0.5 A_d \Delta P_i \mu D_s = C_i \Delta P_i \tag{6}$$

where $C_i = (\pi/8)\mu D_v^2 D_s$, μ is the friction coefficient of the bearing area, and D_s indicates the stem diameter of the valve. Note that we need to fit suitable curves on c_v and R_{ni} for analytical modeling of the system; both the coefficients are functions of the valve rotation angle and hence are needed to be formulated for the analytical modeling and the nonlinear dynamic analysis (stability analysis) [2] which will be carried out for the next phase of the research. For our case study of $D_v = 8$ in., the valve coefficient and resistance are formulated with the aid of the following functions:

$$c_v(\alpha_i) = a\alpha_i^3 + b\alpha_i^2 + c\alpha_i + d \tag{7}$$

$$R_{ni}(\alpha_i) = \frac{7.2\times 10^5}{(a\alpha_i^3 + b\alpha_i^2 + c\alpha_i + d)^2} \tag{8}$$

where $a = 461.9$, $b = -405.4$, $c = -1831$, and $d = 2207$. Clearly, the mass continuity principle implies $q_{in} = q_{out} = q_v$. Rewriting Eq. (4) yields

$$\frac{P_{in} - P_1}{R_{n1}(\alpha_1)} = \frac{P_2 - P_{out}}{R_{n2}(\alpha_2)} \tag{9}$$

$$R_{n1}P_2 + R_{n2}P_1 = R_{n2}P_{in} + R_{n1}P_{out} \tag{10}$$

Combining Eqs. (1) and (10) gives

$$P_1(R_{n1}, R_{n2}, R_L) = \frac{R_{n2}P_{in} + R_{n1}P_{out} + R_{n1}R_L q_v}{(R_{n1} + R_{n2})} \tag{11}$$

$$P_2(R_{n1}, R_{n2}, R_L) = \frac{R_{n2}P_{in} + R_{n1}P_{out} - R_{n2}R_L q_v}{(R_{n1} + R_{n2})} \tag{12}$$

Based on Eqs. (11) and (12), we can explain the roles of R_{n1}, R_{n2}, and R_L on the variations of P_1 and P_2 with the given values of P_{in}, P_{out}, and q_v, as observed in the practice. On the other hand, the downstream valve is too sensitive to any even slight change of the upstream valve dynamics. We hence can rewrite both the hydrodynamic and bearing torques dependency on all the resistances as follows:

$$T_{hi} = f_i(\alpha_i) D_v^3 \Delta P_i(R_{n1}, R_{n2}, R_L) \tag{13}$$

$$T_{bi} = C_i \Delta P_i(R_{n1}, R_{n2}, R_L) \tag{14}$$

Applying the moment equation for both the valves, the equations of motion are written as follows; for the actuated system, the magnetic forces ($F_{mi} = (C_{2i}N_i^2 i_i^2/2(C_{1i} + C_{2i}(g_{mi} - x_i))^2)$) [1] are utilized in driving the valves where the holding torques (T_{hoi}) are replaced for the unactuated case

$$\begin{aligned} J_1\ddot{\alpha}_1 + b_{d1}\dot{\alpha}_1 + K_{t1}\alpha_1 = {} & \left[\frac{R_{n1}P_{in} - R_{n1}P_{out} - R_{n1}R_L q_v}{(R_{n1}+R_{n2})}\right] \\ & \times \left[\frac{16T_{c1}}{3\pi\left(1 - \dfrac{C_{cc1}(1-\sin(\alpha_1))}{2}\right)^2} D_v^3 - \frac{\pi}{8}\mu D_v^2 D_s \times \mathrm{sign}(\dot{\alpha}_1)\right] \\ & + \frac{rC_{21}N_1^2 i_1^2}{2(C_{11} + C_{21}(g_{m1} - x_1))^2} + T_{d1} \end{aligned} \tag{15}$$

$$\begin{aligned} J_2\ddot{\alpha}_2 + b_{d2}\dot{\alpha}_2 + K_{t2}\alpha_2 = {} & \left[\frac{R_{n2}P_{in} - R_{n2}P_{out} - R_{n2}R_L q_v}{(R_{n1}+R_{n2})}\right] \\ & \times \left[\frac{16T_{c2}}{3\pi\left(1 - \dfrac{C_{cc2}(1-\sin(\alpha_2))}{2}\right)^2} D_v^3 - \frac{\pi}{8}\mu D_v^2 D_s \times \mathrm{sign}(\dot{\alpha}_2)\right] \\ & + \frac{rC_{22}N_2^2 i_2^2}{2(C_{12} + C_{22}(g_{m2} - x_2))^2} + T_{d2} \end{aligned} \tag{16}$$

Table 1 The system parameters

μ_f	0.018	L	3 m
ρ	$1000\,\mathrm{kg/m^3}$	v	3m/s
μ	0.1	P_{in}	4.5 kPa
$J_{1,2}$	$0.104\times10^{-1}\,\mathrm{kg\cdot m^2}$	$b_{d1,2}$	$2.2\,\mathrm{N\cdot m\cdot s/rad}$
N_i	3300	C_{1i}	$1.56\times10^6\,\mathrm{H^{-1}}$
g_{mi}	0.1 m	V_i	24 V
r	0.05 m	D_v	8 in.
D_s	0.5 in.	P_{out}	0.1 kPa
k	20 kN m	C_{2i}	$6.32\times10^8\,\mathrm{H^{-1}}$
R_i	$6\,\Omega$	$T_{ho1,2}$	$1900\,\mathrm{N\cdot m}$

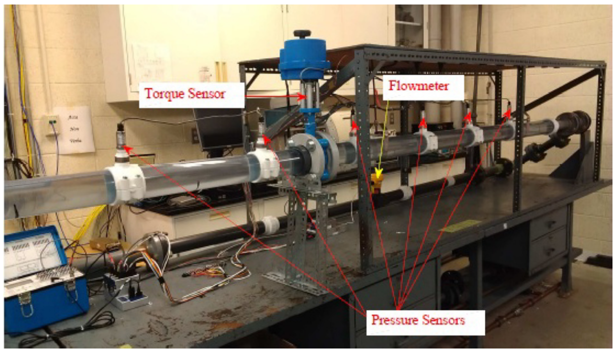

Fig. 2 The experimental work for a set of the actuated butterfly valve

We also utilized the rate of current based on the following equation:

$$\frac{di_i}{dt}=\frac{(V_i-R_ii_i)(C_{1i}+C_{2i}(g_{mi}-x_i))}{N_i^2}-\frac{C_{2i}i_i\dot{x}_i}{(C_{1i}+C_{2i}(g_{mi}-x_i))} \tag{17}$$

where x indicates the plunger displacement, r is the radius of the pinion, F_m stands for the motive force, C_1 and C_2 are the reluctances of the magnetic path (without airgap) and airgap, respectively, N is the number of coil, i indicates the applied current, g_m is the nominal airgap, J is the polar moment of inertia of the valve's disk, b_d is the equivalent torsional damping, K_t indicates the equivalent torsional stiffness, T_d is the disturbance torque, V is the supply voltage, R indicates the electrical resistance of coil, and $\dot{x}$ is the plunger velocity. Equations (15)–(17) constitute the sixth-order dynamic model for the coupled valves.

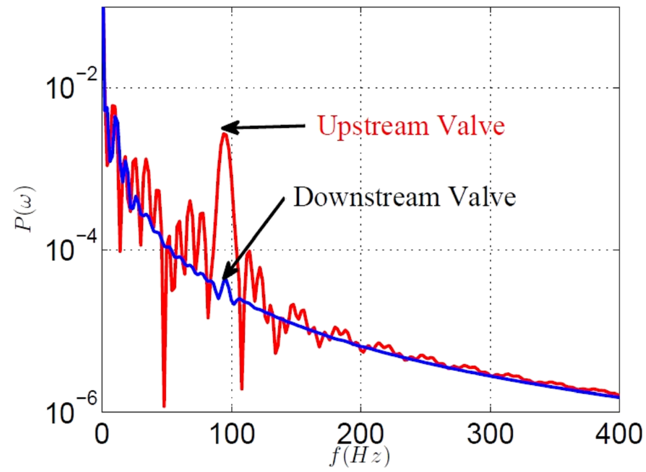

Fig. 4 The valves' power spectra

3 Results

Developing a MATLAB code, a numerical analysis is carried out using the values shown in Table 1 and gathered from the experimental work we have done for a set of the valve/actuator, shown in Fig. 2. We examine the system actuated using the solenoid ones to drive the valves to a certain opening angle and without actuation by applying constant torques to hold the valves at a steady position. For both the cases, a limited periodic noise ($T_{d1}=a\sin(\omega t)$ and $T_{d2}=0$) is applied on the upstream valve to present and discuss the coupling.

3.1 With Actuation. We apply the noise of $T_{d1}=10^3\sin(600t)$ (N·m) for the time interval of $0.03\,\mathrm{s}\le t\le 0.12\,\mathrm{s}$. We intentionally select the time range within the transient phases of the valves' motions. This would give us a clear map of what is expected to occur for the moving valves subject to the noise. Applying the same currents ($i_{1,2}=4$ A) for the valves' fully open positions ($\alpha_{10,20}=0$), Fig. 3(*a*) shows the upstream valve subject to the periodic noise causing small periodic oscillations for the downstream valve. Note that these oscillatory motions occur during the closing process. It is of great interest to capture such a coupling between the valves particularly knowing that tens of valves are operating in the network.

Figure 3(*b*) presents the valves' angular velocities exhibiting the same frequency but smaller amplitudes of the downstream valve with respect to the noise applied on the upstream one. The power spectrum is one of the tools from nonlinear dynamic

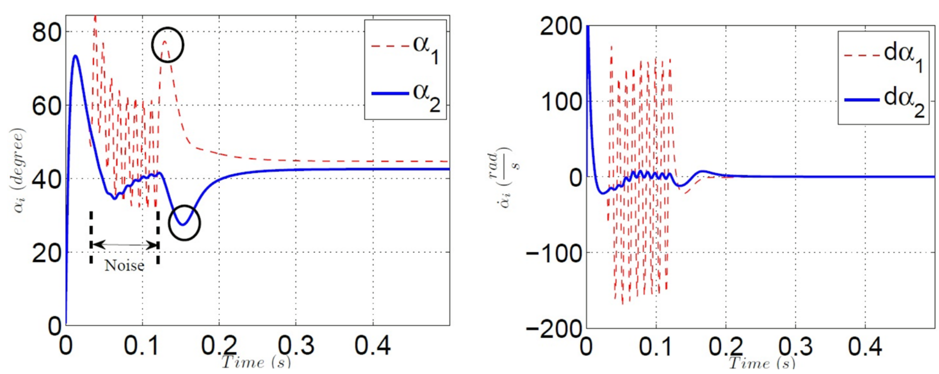

(a) (b)

Fig. 3 (*a*) The actuated valves' motions versus time. (*b*) The actuated valves' angular velocities versus time.

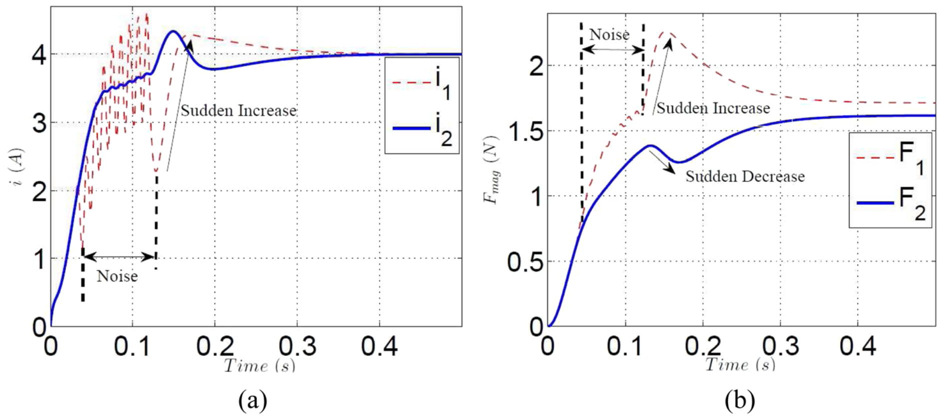

Fig. 5 (*a*) **The rates of currents for the noise applied on the upstream valve. (*b*) The magnetic forces for the noise applied on the upstream valve.**

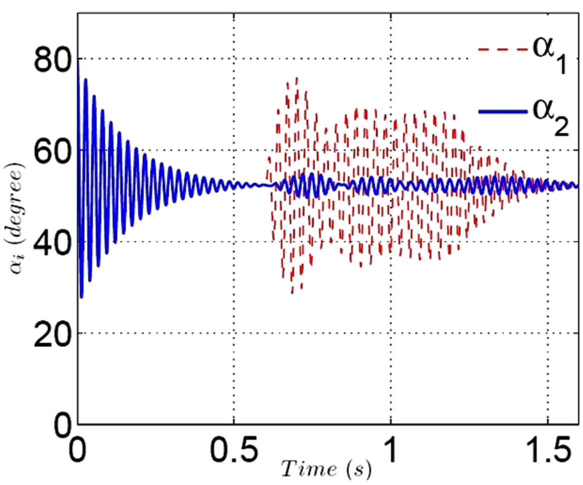

Fig. 6 The unactuated valves' motions versus time

analysis helping us clarify the motion of the downstream valve. Figure 4 presents the valves' power spectra revealing the same frequencies ($\omega = 600\text{rad/s}$) to confirm that the downstream valve follows the periodic motion applied on the upstream one with smaller amplitudes.

We discussed the coupling between the valves though another interaction exists between the actuators where the rack and pinion transfers the valve motion to the solenoid plunger.

Note that the current depends on both the valve rotation angle (the plunger displacement) and angular velocity (the plunger velocity), as stated in Eq. (17). The same oscillatory behavior of either the valve rotation angle or angular velocity is hence expected to be observed for the rates of currents shown in Fig. 5(*a*). This is of great interest to capture the coupling between the actuation parts due to the noise applied on the valve. We also expect the same behavior of the magnetic force shown in Fig. 5(*b*) in connection with the current based on the above mentioned relationship.

The flow between the valves and modeled as a resistor, on the other hand, transfers any change of the upstream to the downstream valve. Figure 3(*a*) reveals a sudden increase and decrease, at the end of the time interval ($t = 0.12\,\text{s}$), in both the upstream and downstream valves' angles, respectively, presented by two circles. These interesting phenomena can be interpreted as follows. The noise applied on the upstream valve oscillates the current (as discussed earlier) affecting the magnetomotive force. Removing the noise, both the current and magnetic force increase rapidly, as expected and shown in Figs. 5(*a*) and 5(*b*) by arrows, causing the sudden increase observed for the upstream valve angle.

The rapid increase of the upstream valve angle accelerates the flow between the valves which results in a higher value of the flow force hitting the downstream one. The accelerated and shock-like flow force opposes the downstream valve to be closed and consequently the valve angle decreases for a short period of time. Note that the current of the downstream set rises (for the short period of time) though its magnetic force reduces such that the role of the valve angle, in comparison with the current, is more drastic in increasing the denominator of the force term.

3.2 Without Actuation. In Sec. 3.1, we illustrated the coupling between the valves moving toward the certain angles. We here investigate the valves' interactions to be held at a steady position with the aid of the holding torques. The valves are released from an initial angle, say 80 deg, and gradually settle down with respect to the amounts of the applied constant torques. We again exert a limited periodic noise on the upstream valve at its steady position.

Applying $T_{\text{ho1}} = T_{\text{ho2}} = 1900\,(\text{N}\cdot\text{m})$ and the noise of $T_{\text{d1}} = 150\sin(200t)(\text{N}\cdot\text{m})$ for $0.6\,\text{s} \le t \le 1.2\,\text{s}$, Fig. 6 shows both the transient phase ending at $t = 0.6\,\text{s}$ and the steady position subject to the noise. Note that we reduce the value of the torsional damping ($b_{\text{t1,2}} = 0.5\,\text{N}\cdot\text{m}\cdot\text{s/rad}$) in order to magnify both the phases and the coupling. The downstream valve again follows the motion of the upstream one (the same frequency) with smaller amplitudes but larger than those of the moving case.

Figure 6 also reveals the fluctuating (increasing and decreasing) amplitudes of the upstream and accordingly the downstream valves due to the noise. The physical interpretation of this phenomenon is as follows. The applied noise oscillates the upstream valve until it reaches its closing position with the aid of the helping hydrodynamic torque [3]. At this point, the powerful and resisting bearing torque [3] takes an important role to push back the valve and hence the amplitude decreases. Note that the bearing torque is too sensitive to the pressure drop across the valve and we hence expect a remarkable value of the torque for $\alpha_1 > 60\,\text{deg}$; we have carried out an experimental work with the valve diameter of $D_{\text{v}} = 2$ in. (Fig. 2) presenting a sharp jump of the pressure drop shown in Fig. 7(*a*) for the angles higher than that of 60 deg. Note that the experiment was repeated several times to yield reliable data. The amplitude hence reduces until the dominant hydrodynamic torque, as a helping factor for $\alpha_1 < 60\,\text{deg}$, increases it. Using a torque sensor, we also recorded the experimental values of the total acting torque shown in Fig. 7(*b*) exhibiting the remarkable values of the resisting torque (the dominant bearing torque)

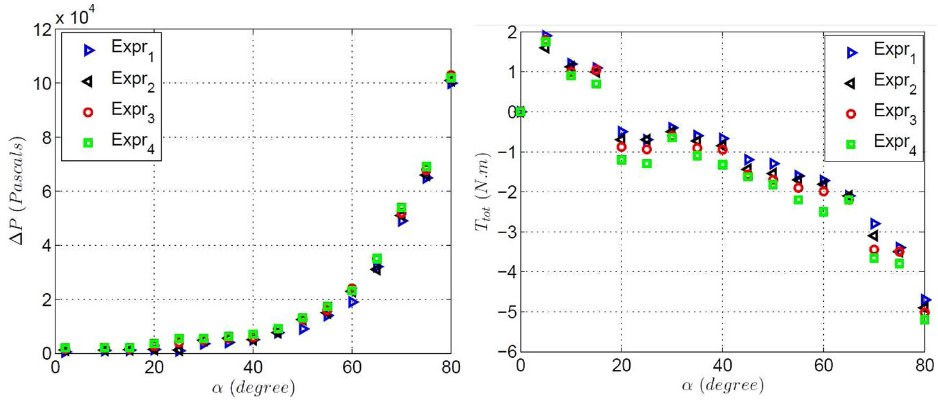

(a) (b)

Fig. 7 (*a*) The experimental pressure drop revealing a sharp jump for $\alpha > 60$ deg; a set of the valve/actuator. (*b*) The experimental total torque for a set of the valve/actuator.

to oppose the valve motion. Obviously, the fluctuations gradually vanish when we remove the noise.

4 Conclusions

This paper focused on the nonlinear analysis of two solenoid actuated butterfly valves coupled in series. We modeled the system by making some simplifying assumptions. The dependency of the valves' pressure drops on the varying (R_{n1} and R_{n2}) and constant (R_L) resistors were then established. The most important flow nonlinear torques including the hydrodynamic and bearing torques were reformulated and then the equations of motion developed.

We applied a periodic noise on the upstream valve to capture the couplings of the valves and the actuation parts. For the actuated system, the downstream valve followed the oscillation of the upstream one (the same frequency) with smaller amplitudes. The shown power spectra support such a behavior of the downstream valve.

The unactuated valves' couplings were then investigated by applying the holding torques to keep the valves at a steady position. Surprisingly, we captured the remarkable roles of the hydrodynamic and bearing torques to fluctuate both the upstream (the source of the noise) and downstream valves' amplitudes. The sensitive bearing torque to the pressure drop pushes back the valve for the angles higher than that of 60 deg and the helping hydrodynamic torque increases the amplitude of the oscillation for $\alpha_1 < 60$ deg. Note that the pressure drop experiences a sharp jump for $\alpha_1 > 60$ deg; the experimental work we have carried out validates the sharp jump of the pressure drop.

We currently focus on capturing dangerous behaviors including chaos and crisis for a set of critical parameters of the coupled system.

Acknowledgment

The author is grateful to Professor C. Nataraj, the Chairman of Mechanical Engineering Department at Villanova University, for his genuine and novel ideas. The experimental work was supported by Office of Naval Research Grant No. N00014/2008/1/0435.

References

[1] Naseradinmousavi, P., and Nataraj, C., 2011, "Nonlinear Mathematical Modeling of Butterfly Valves Driven by Solenoid Actuators," J. Appl. Math. Modell., **35**(5), pp. 2324–2335.

[2] Naseradinmousavi, P., and Nataraj, C., 2012, "Transient Chaos and Crisis Phenomena in Butterfly Valves Driven by Solenoid Actuators," Commun. Nonlinear Sci. Numer. Simul., **17**(11), pp. 4336–4345.

[3] Naseradinmousavi, P., and Nataraj, C., 2013, "Optimal Design of Solenoid Actuators Driving Butterfly Valves," ASME J. Mech. Des., **135**(9), p. 094501.

[4] Kwuimy, C. A. K., and Nataraj, C., 2012, "Modeling and Dynamic Analysis of a Magnetically Actuated Butterfly Valve," Nonlinear Dyn., **70**(1), pp. 435–451.

[5] Seman, A., 2007, "Adaptive Automation for Machinery Control," ONR Presentation.

[6] Hughes, R., Balestrini, S., Kelly, K., Weston, N., and Mavris, D., 2006, "Modeling of an Integrated Reconfigurable Intelligent System (IRIS) for Ship Design," Proceedings of the ASNE Ship and Ship Systems Technology (S3T) Symposium.

[7] Automation, F., 2011, DDG-51 Class Chilled Water Automation Systems (CWAS) Land-Based Performance Test (LBPT) Facility Control and Monitoring System (CMS).

[8] Schweitzer, G., Bleuler, H., and Traxler, A. H., 1994, *Active Magnetic Bearing, Basics, Properties and Applications of Active Magnetics Bearings*, Verlag der Facvereine (vdf).

[9] Preumont, A., 2006, *Mechatronics: Dynamics of Electromechanical and Piezoelectric Systems*, Springer, New York.

[10] Heisler, I. A., Braun, T., Zhang, Y., Hu, G., and Cerdeirax, H. A., 2003, "Experimental Investigation of Partial Synchronization in Coupled Chaotic Oscillators," Chaos, **13**(1), pp. 185–195.

[11] Ge, Z. M., and Lin, T. N., 2003, "Chaos, Chaos Control and Synchronization of Electro-Mechanical Gyrostat System," J. Sound Vib., **259**(3), pp. 585–603.

[12] Siewe, M. S., Yamgoue, S. B., Kakmen, F. M. M., and Tchawoua, C., 2010, "Chaos Controlling Self-Sustained Electromechanical Seismograph System Based on the Melnikov Theory," Nonlinear Dyn., **62**, pp. 379–389.

[13] Ho, J. H., Nguyen, V. D., and Woo, K. C., 2011, "Nonlinear Dynamics of a New Electro-Vibro-Impact System," Nonlinear Dyn., **63**, pp. 35–49.

[14] Brauer, J. R., 2006, *Magnetic Actuators and Sensors*, Wiley, Hoboken, NJ.

[15] Sarpkaya, T., 1959, "Oblique Impact of a Bounded Stream on a Plane Lamina," J. Franklin Inst., **267**(3), pp. 229–242.

[16] Sarpkaya, T., 1961, "Torque and Cavitation Characteristics of Butterfly Valves," ASME J. Appl. Mech., **28**(4), pp. 511–518.

[17] Park, J. Y., and Chung, M. K., 2006, "Study on Hydrodynamic Torque of a Butterfly Valve," ASME J. Fluids Eng., **128**(1), pp. 190–195.

[18] Wikipedia, 2014, Hagen–Poiseuille Equation—Wikipedia, The Free Encyclopedia, accessed June 24, 2014.

[19] Association, A. W. W., 2012, *Butterfly Valves: Torque, Head Loss, and Cavitation Analysis*, 2nd ed., American Water Works Association, Denver, CO.

[20] Leutwyler, Z., and Dalton, C., 2008, "A CFD Study of the Flow Field, Resultant Force, and Aerodynamic Torque on a Symmetric Disk Butterfly Valve in a Compressible Fluid," ASME J. Pressure Vessel Technol., **130**(2), p. 021302.